NANOSTRUCTURING OF LASER TEXTURED SURFACE TO ACHIEVE SUPERHYDROPHOBICITY ON ENGINEERING METAL SURFACE

Paper # P103

Avik Samanta[1], Qinghua Wang[1], Scott K. Shaw[2], Hongtao Ding[1,*]

[1] Department of Mechanical Engineering, University of Iowa, Iowa City, Iowa 52242, USA
[2] Department of Chemistry, University of Iowa, Iowa City, Iowa 52242, USA

Abstract

Superhydrophobic metal alloy surfaces are increasingly employed in aerospace and naval applications for anti-icing, drag reduction, self-cleaning, and high-efficiency light absorption capabilities. Emerging laser-based surface texturing methods demonstrate significant potential for manufacturing these surfaces, with the advantages of high processing precision and flexibility. In this research, superhydrophobicity is achieved on engineering metal surfaces using a novel nanosecond Laser-based High-throughput Surface Nanostructuring (nHSN) process. First, a high-energy nanosecond pulse laser scans the metal surface submerged in water using a large spatial increment and a fast processing speed. After that, the laser-textured surface is further treated by immersion in a chlorosilane reagent for a specific period of time. As a result of these two processes, micro- and nano-scale surface features are generated on the metal surface. These features are measured on AISI 4130 steel workpieces through X-ray Photoelectron Spectroscopy (XPS) and Scanning Electron Microscopy (SEM) and correlated with processing conditions. The features are also compared after completion of each process step to understand their individual and cumulative effect on the textured surface. It is found that utilizing a high laser power intensity during the laser texturing process phase will significantly enhance surface nanostructuring effects after the chlorosilane treatment, resulting in feature size decrease and increase in feature density.

Keywords

Surface Texturing, Nanosecond Laser, Nanostructuring, Superhydrophobicity, Chlorosilane.

Introduction

Recently, functional engineering surface has attracted the attention of researchers due to their great potential for multi-functional applications. One of the prime examples of multi-functional surfaces is [1]superhydrophobic metal alloy surfaces that are increasingly employed in aerospace and naval applications. Superhydrophobic phenomenon was first discovered on plant leaves [1], insect legs [2] and wings [3], while people have spent decades on the biomimetic trail. Superhydrophobic surface has some excellent surface properties for anti-icing [4–7], drag reduction [8–11], anticorrosion [12,13], self-cleaning [14–16], anti-biofouling [17,18], and high-efficiency light absorption capabilities [19–22]. Drag reduction, anticorrosion, anti-biofouling, and anti-icing properties of superhydrophobic metal surfaces are utilized for marine surfaces to extend their lives especially in extreme cold arctic regions [23]. Modern aerospace industry deploys the anti-icing, self-cleaning and solar light absorption capabilities of hydrophobic surfaces for future solar aircraft [24]. Three main techniques are widely used to prepare superhydrophobic multifunctional surface; (a) top-down approach which removes material from bulk workpiece to create nanoscale structures using energy sources, chemical and electrochemical processes [14–16,22]; (b) bottom-up approach which builds up nanoscale features though nano-manufacturing from atomic and molecular-scale components [25,26]; and (c) a combination of top-down and bottom-up approach [27]. The top-down approach is comparatively faster and economically feasible process for industrial application.

Emerging laser-based surface texturing methods demonstrate significant potential for manufacturing functional surfaces, with the additional advantages of maintaining high precision and process flexibility. Existing laser-based surface-texturing methods often employ ultra-short pulse lasers to generate micro-scale patterns or periodic nanoscale features on metallic materials [14,16,20,21,28–45]. Considerable investigation has been afforded two primary ultra-short laser-based surface texturing methods: (1) laser-induced

*Corresponding author: hongtao-ding@uiowa.edu

periodic surface structure (LIPSS) consisting of laser-induced surface ripples with periodicity equal to or smaller than the wavelength of the laser radiation [21,29,30]; and (2) laser surface inscribing to achieve hierarchical structures consisting of ordered microstructures (e.g., parallel microgrooves) [15,22,36,40]. To create these surface structures, both methods scan metal surfaces at a very fine spatial resolution for which a long processing time for a given unit of area is required. Extensive research in the past decade has shown that a metal surface textured using ultra-short laser scanning is inherently hydrophilic [35,38,39].

In order to achieve a hydrophilicity-to-superhydrophobicity transition, the chemical composition of the laser-textured surface must be altered to reduce surface energy. Various post-laser process methods have been applied to ultra-short laser pre-textured metal surfaces, including a chemical surface treatment process [33–35] or a long-term storage period (characteristically in air for several weeks) [14,16,32,33,38,39,45]. Steele et al. [33] fabricated LIPSS consisting of cone-like microstructure on pure titanium substrates using a femtosecond pulse laser with subsequent application of fluoropolymer coating on top of the laser textured surface. These results showed that the laser-textured surface with fluoropolymer coating exhibited superhydrophobicity with a contact angle of 165°. Vorobyev and Guo [15], experimenting with platinum, titanium, and brass, used a femtosecond pulse laser to create omnidirectional microgrooves consisting of hierarchical microstructures. Specimens reportedly achieved hydrophilicity immediately after femtosecond laser surface structuring but required long exposure in air to achieve superhydrophobicity. The transition occurred predominantly due to chemical interaction between the surface and the ambient CO2, resulting in an accumulation of carbon and carbon compounds on the laser-treated surface. Martinez-Calderon et al. [36] investigated the wetting behavior for AISI 304 stainless steel alloy for different types of surface structures using a femtosecond pulse laser, including omnidirectional trenches, cross-hatch trenches, omnidirectional trenches covered by LIPSS and cross-hatch trenches covered by LIPSS. An additional laser-texturing step was required to create LIPSS over the microstructured specimens. All specimens subject to femtosecond laser texturing were hydrophilic, with an initial contact angle less than 30° directly after laser treatment. After storing in air for more than 120 hours, these surfaces became hydrophobic and superhydrophobic for microstructured (omnidirectional or cross-hatch trenches) specimens and hierarchical structured (omnidirectional or cross-hatch trenches covered with LIPSS) specimens, respectively.

It should be emphasized that these state-of-the-art surface treatment methods rely on a laser-texturing phase to generate surface micro-/nanoscale features. Surface nanostructuring effects have never been observed in any of these existing post-laser processes. It is generally believed that silane-based surface modification treatments provide only a surface coating effect, for which etching in metal alloys would not occur during post-processing subsequent to ultra-short laser texturing. In contrast to this conventional understanding of surface silanization, this study shows that chemical surface treatment induces simultaneous silanization effects and significant chemical etching for metal surfaces prepared using laser texturing.

Experimental Procedure

A novel nanosecond Laser-based High-throughput Surface Nanostructuring (nHSN) process is developed for engineering metal alloys to achieve superhydrophobic surfaces. This novel process consists of two steps: (1) water-confined nanosecond laser texturing, during which a high energy nanosecond pulse laser scans the material surface contained under water using a large spatial increment and a fast processing speed, (2) chemical immersion treatment, during which the laser textured surface is further chemically treated.

Water confined Nanosecond Laser Texturing

The experimental setup for the water confined nanosecond laser texturing tests uses a Q-Switched Nd:YAG nanosecond laser (Spectra-Physics Quanta-Ray Lab-150, wavelength 1064 nm) with a high energy per pulse on the order of several hundreds of mJ/pulse. During the laser texturing process, the laser repetition rate is 10 pulses per second with a laser pulse duration of 6~8 ns. A galvanometer laser scanner (SCANLAB intelliSCAN® 20) furnished with an f-theta objective with a focal length of 255 mm directs the laser to texture the top surface of the specimen. The specimen is submerged in deionized water, which confines the laser pulse-induced plasma and enhances the texturing effect.

Figure *1*a shows the schematic representation of the water-confined nanosecond laser texturing system. The workpiece is kept under deionized water confinement (around 8 mm depth from the specimen surface) in a tank, which is positioned using computer-controlled stages. Figure *1*b shows the typical laser scanning path used during the experiments. The laser scan head scans the top surface of the work material in a zig-zag pattern as shown in Figure *1*b. The X-spacing (or pitch) defines the distance between two sequential laser scan lines and

is pre-set through computer control. The Laser Scan Line Density, as determined by Eq. 1, defines how many laser scan lines are required to scan a 1-inch width area. The Y-spacing between two sequential laser shots along the scanning direction is determined by the Laser Repetition Rate and pre-set Laser Scanning Speed as in Eq. 2. The Overlap Ratio is set by the ratio of Overlap Area to the Laser Spot Area as in Eq. 3. For all the experimental conditions in this study, a same value was applied for both X-spacing and Y-spacing, which guarantees the same Overlap Ratio of 50% in both directions. The Laser Spot Area can be adjusted by moving the Z stage away from the focal plane.

$$\text{Laser Scan Line Density (lines/in)} = \frac{1\text{ in}}{\text{X} - \text{spacing}} \quad (1)$$

$$\text{Y} - \text{spacing} = \frac{\text{Laser Scanning Speed}}{\text{Laser Repetition Rate}} \quad (2)$$

$$\text{Overlap Ratio} = \frac{\text{Overlap Area}}{\text{Laser Spot Area}} \times 100\% \quad (3)$$

The combination of laser scan head and computer-controlled stages allows to have a wide range of laser scanning area during the process. Both laser and scan head are controlled by a microcontroller for scanning along a pre-designed path. The scan head is also connected to a water cooling system to avoid any undesirable heating of the scan head during the process.

Chemical Immersion Treatment

After the laser texturing, the workpieces were immersed in an ethanol solution with 1.5% volume percentage cholosilane reagent [$CF_3(CF_2)_5(CH_2)_2SiCl_3$], also known as FOTS at room temperature for ~3 hours as shown in Figure *1*c. Workpieces were then cleaned with deionized water and dried using compressed air. Finally, it was kept at 80 °C in a vacuum oven for 1 hour to dry it out completely.

Measurements and Characterization

Water Contact Angle for the treated specimen surface was measured during the wettability test using a contact angle goniometer (Rame-Hart model 100) coupled with a high-resolution CMOS camera (6~60× magnification, Thor Laboratories). For each WCA measurement, about 4 μL volume of water was dropped to form a still water droplet on the specimen surface, and its optical shadowgraph was obtained using the CMOS camera. The optical shadowgraph was quantitatively analyzed using ImageJ software to determine the WCA for each measurement. Multiple WCA measurements were performed at various locations inside each specimen surface, and the average value of measurement results was obtained.

The surface morphology of the superhydrophobic surface was analyzed using scanning electron microscope (Hitachi S-4800). The SEM images were taken at 1.8-2.0 kV acceleration voltages. Additionally, XPS analysis was carried out for the surface chemistry using Kratos Axis Ultra high-performance X-ray Photoelectron Spectroscopy system. To investigate the chemical composition at a certain depth, the surface was etched by 100 nm by ion-gun etching cycles between two adjacent XPS measurements. Full survey spectra and high-resolution elemental spectra were acquired for surface composition analysis and chemical state identification, respectively.

Results and Discussions

Water Contact Angle

The wettability of the specimen surface produced by developed process was experimentally evaluated through water wetting tests. The definition of surface wettability can be described as the tendency of a liquid to spread on or adhere to a solid surface without the formation of droplets. When the liquid is water, it completely wets the hydrophilic surface without the formation of droplets; while water droplets will form on hydrophobic surfaces. Water contact angle (WCA) is one of quantitative method to define how water interacts with a solid surface without absorbing the water, dissolving in the water or reacting with the water. It is defined as the angle, conventionally measured through the water droplet, where water–vapor interface meets a solid surface and can be used to quantify the wettability of a solid surface.

As illustrated in Figure 2a, the surface wettability to water can be categorized into four categories: hydrophobic, hydrophilic, superhydrophobic and superhydrophilic. If WCA is less than 30°, the surface is designated superhydrophilic, and the water completely spreads over the surface. If the WCA is in between 30° and 90°, the surface is categorized as hydrophilic. On a hydrophobic surface, water forms distinct droplets. As the hydrophobicity increases, the contact angle of the droplets with the surface increases. Surfaces with WCA greater than 90° are designated as hydrophobic. When WCA is greater than 150°, the surface is generally regarded as superhydrophobic.

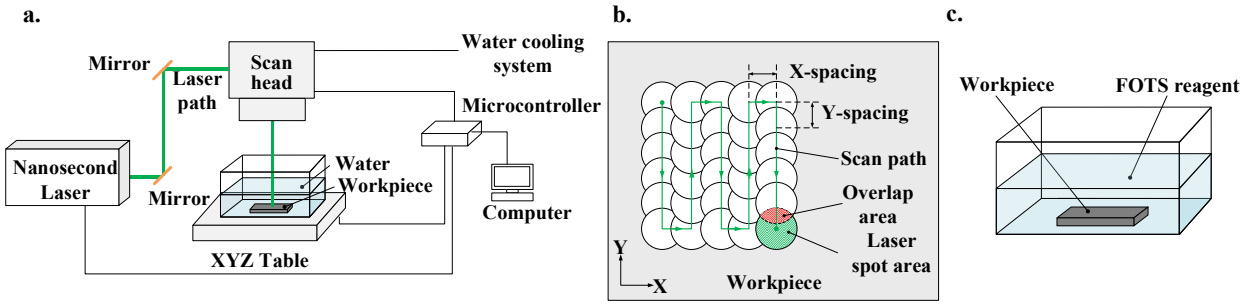

Figure 1: Schematic representation of the process: (a) experimental setup of water-confined nanosecond laser texturing; (b) laser scanning path; (c) experimental setup of chemical immersion treatment.

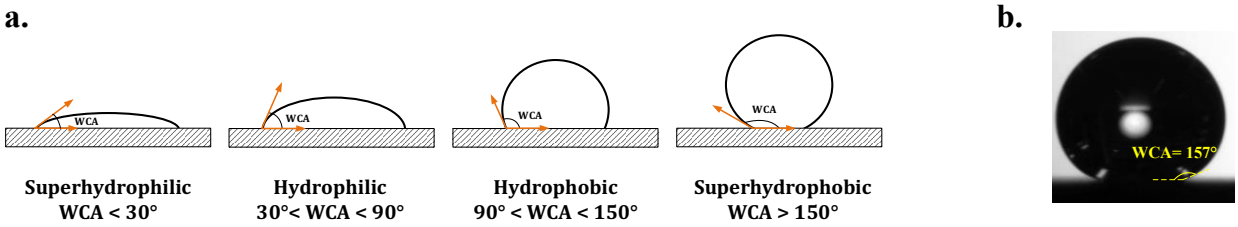

Figure 2: (a) Schematic representation of four exemplary scenarios of Water Contact Angle (WCA). (b) Measured WCA in the superhydrophobic AISI 4130 steel surface.

Figure 2b illustrates the sprayed water droplets formed on the AISI 4130 steel specimen surface treated by the process developed in this study. It can be noted that completely spherical water droplets form on the processed surface, demonstrating the superhydrophobicity. Figure 3 shows the water contact angle measurement results for AISI 4130 steel specimens produced by the laser surface texturing process using various laser power intensities ranging from 0.1 to 18.2 GW/cm^2. The uncertainty was typically around ±2° for each test. The measurement for 0 GW/cm^2 was performed on the specimens produced by the chemical immersion treatment alone without any prior laser texturing, and their results show a WCA of 96.9°. The specimens treated by low laser power intensities from 0.1 GW/cm^2 during the laser texturing step showed improved hydrophobicity with increased WCA up to 111.1°. These tests also indicated that a higher laser power intensity helped increase the WCA during the process. Further increase in laser power intensity during the texturing process improved the WCA in the superhydrophobic range. All the specimens treated by laser power intensities from 0.2 to 18.2 GW/cm^2 achieved superhydrophobicity with WCA greater than 150°. Varying laser power intensity did not significantly alter the WCA for these superhydrophobic AISI 4130 steel specimens. These results indicated that a wide process window existed to produce consistent superhydrophobic AISI 4130 steel surfaces, as long as the laser power intensity was equal or greater than 0.2 GW/cm^2.

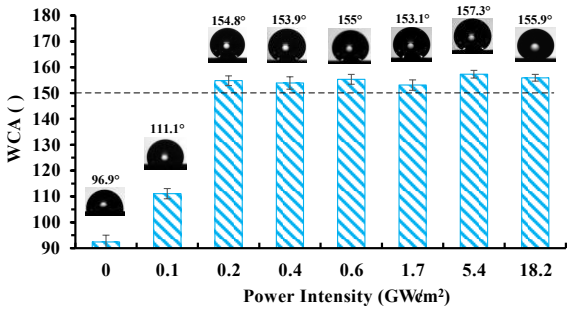

Figure 3: Contact angle measurement results for AISI 4130 steel specimens produced by the nHSN process at various laser power intensities ranging from 0 (indicating no laser texturing and only chemical immersion treatment) to 18.2 GW/cm^2.

Surface Nanostructure

The surface microstructures were analyzed for various specimens directly after the laser texturing and after the chemical treatment as illustrated in Figure 4. In this study, the specimens were processed by same laser power intensity of 0.6 GW/cm^2. Therefore, only difference between the two samples was that one went through the chemical immersion treatment while the other did not. Micrographs at different magnification

ranging from 100× to 20,000× were shown in Figure 4. In comparison, at 100× magnification with a view area of about 1 mm^2, both the specimens show an isotropic texture. There is no significant difference between the surfaces without any obvious lay pattern as shown in Figure 4a and d. At 5000× magnification, significantly different surface microstructures can be observed as illustrated in Figure 4b and e. Numerous tiny pores, and thermal cracks and microscale ripples can be observed immediately after laser texturing whereas spherical micro-/nano-structures were homogenously distributed over the other specimen that underwent chemical immersion treatment after laser texturing. The microscale ripples were induced from the nanosecond laser-steel interaction under water confinement on the specimen after laser texturing, which were not observed after chemical immersion treatment. This indicated the chemical immersion treatment significantly modified the surface morphology. At 20000× magnification with a view area of about 30 µm2, the pores and thermal cracks were more clearly observed in Figure 4c on the specimen with only laser texturing. Whereas, nanoscale spherical protrusions, rods, cones, platelets, and pores with size of few hundreds of nanometers are observed on the sample which went through chemical immersion treatment after laser texturing (Figure 4f).

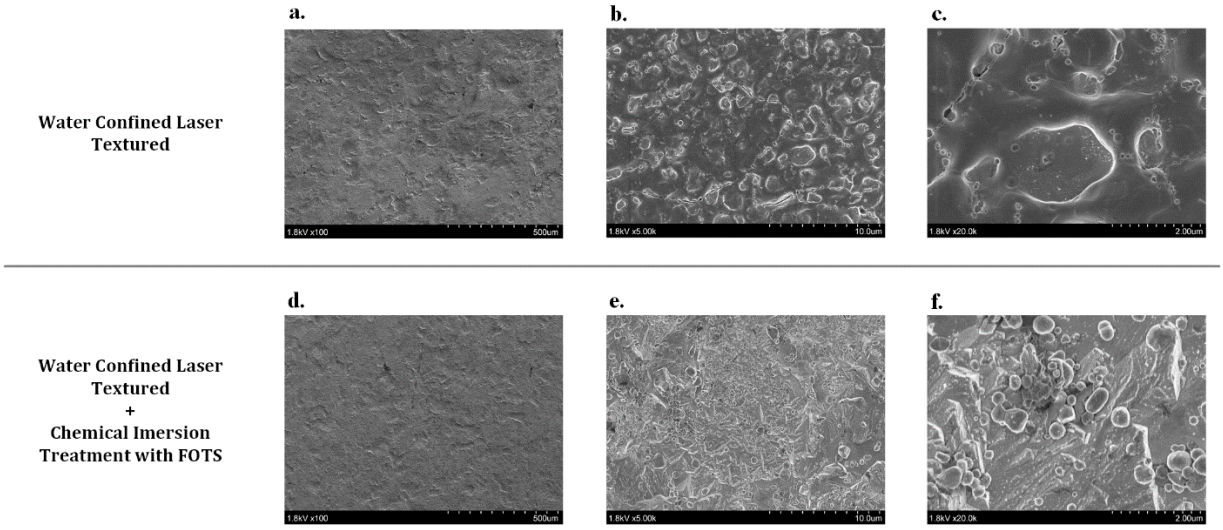

Figure 4: Scanning electron microscope (SEM) micrographs of two AISI 4130 steel specimens. At top, specimen processed water confined laser texturing with laser power intensity of 0.6 GW/cm^2 at various magnification (a) 100×, (b) 5000× and (c) 20000×. At bottom: specimen processed with chemical immersion treatment after water confined laser texturing with laser power intensity of 0.6 GW/cm^2 at various magnification (d) 100×, (e) 5000× and (f) 20000×.

Chemistry Analysis

The elemental composition of the treated surface was investigated using the X-ray photoelectron spectroscopy (XPS) survey of the surface and at a 100 nm depth as illustrated in Figure 5. It can be observed that immediately after water confined laser texturing, elements such as oxygen, carbon, and iron were detected on the laser textured surface and their corresponding intensities were reduced as the etched depth increased to 100 nm. The iron and carbon came from the composition of AISI 4130 steel and oxygen came from the oxidation/hydroxylation happened during water confined laser texturing (Figure 5a). For the sample which went through both water confined laser texturing and subsequent chemical immersion treatment, significantly different XPS spectra was observed. Two additional peaks in fluorine and silicon along with oxygen, carbon, iron were observed in the survey at the surface (Figure 5b). Those two peaks were completely gone at the etched depth of 100 nm. The source of fluorine and silicon belonged to FOTS cholosilane reagent $[CF_3(CF_2)_5(CH_2)_2SiCl_3]$. $–CF_2$- and $–CF_3$ groups present on the cholosilane structure were attached to the processed surface leading to surface fluorination. $–CF_2$- and $–CF_3$ groups are known to be low binding energy groups, so with their attachment to the surface, surface energy was reduced that contributed to the superhydrophobicity. Surprisingly, no chlorine signal was observed in the XPS survey though there is chlorine in the FOTS reagent. It is hypothesized that the chlorine elements in FOTS cholosilane reagent reacted with metal oxide and dissolved in the chemical solution.

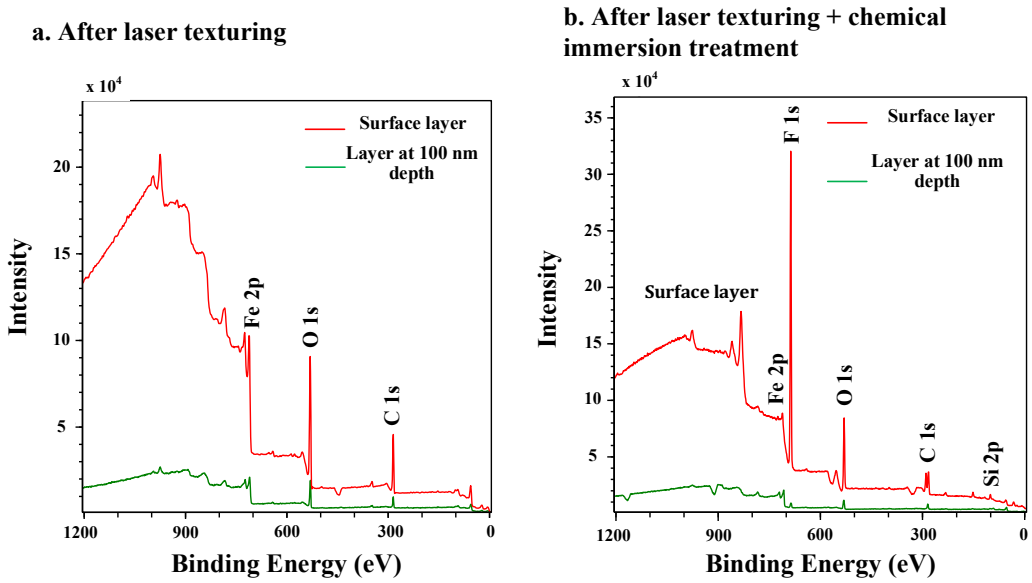

Figure 5: XPS survey of the surface layer and at 100 nm depth for (a) specimen underwent water confined laser texturing and (b) specimen underwent both water confined laser texturing and subsequent chemical immersion treatment with FOTS cholosilane reagent.

After the chemical immersion treatment, post process liquid solution was chemically tested to find out the etched away metal elements in the solution. Sodium hydroxide (NaOH) and deionized water were added to the solution. After sometime, reddish-brown precipitates were formed as shown in Figure 6. From the color of the precipitates, they are believed be Ferric Hydroxide [$Fe(OH)_3$], which is insoluble in water. This definitely proved that etching happened due to chlorine during the chemical immersion treatment that brought Fe elements from substrate to the solution. This finding would contribute to the nanostructure formation as discussed in the previous section.

Reddish-Brown Precipitate
[Post CIT solution for 4130 Steel + NaOH + DI Water]

Figure 6: Chemical analysis to show etching effect that brought Fe elements to the solution.

Conclusions

A novel water confined nanosecond laser texturing method coupled with chemical immersion treatment was successfully developed for producing superhydrophobic AISI 4130 steel surface. The process is completely different from the state of the art laser-induced periodic surface structures produced from existing ultra-short laser-based surface-texturing methods. Wide range of laser power intensities ranging from 0.2 to 18.2 GW/cm^2 were used to produce stable superhydrophobic surface with WCA consistently greater than 150°. Nanoscale surface protrusions, rods, cones, platelets and pores with size of few hundreds of nanometers were observed in microstructure analysis that contributed for superhydrophobicity. Surface chemical analysis was also performed using XPS. It showed the presence of $–CF_2$- and $–CF_3$ groups on the surface, confirming the occurrence of surface fluorination in specimens during chemical immersion treatment. Low binding energy $–CF_2$- and $–CF_3$ groups reduced surface energy and led to an enhancement of surface hydrophobicity.

Acknowledgements

The authors gratefully acknowledge the financial support by the National Science Foundation under Grant Number CMMI-1762353.

References

[1] Darmanin T and Guittard F 2015 Superhydrophobic and superoleophobic properties in nature *Mater. Today* **18** 273–85

[2] Gao X and Jiang L 2004 Water-repellent legs of water striders *Nature* **432** 36

[3] Wagner T, Neinhuis C and Barthlott W 1996 Wettability and Contaminability of Insect Wings as a Function of Their Surface Sculptures *Acta Zool.* **77** 213–25

[4] Bogoslov E A, Danilaev M P, Mikhailov S A and Pol′skii Y E 2016 Energy Efficiency of an Integral Anti-Ice System Based on Fluoroplastic Films *J. Eng. Phys. Thermophys.* **89** 815–20

[5] Cao L, Jones A K, Sikka V K, Wu J and Gao D 2009 Anti-Icing superhydrophobic coatings *Langmuir* **25** 12444–8

[6] Ruan M, Li W, Wang B, Deng B, Ma F and Yu Z 2013 Preparation and anti-icing behavior of superhydrophobic surfaces on aluminum alloy substrates *Langmuir* **29** 8482–91

[7] Boinovich L B, Emelyanenko A M, Emelyanenko K A and Maslakov K I 2016 Anti-icing properties of a superhydrophobic surface in a salt environment: an unexpected increase in freezing delay times for weak brine droplets *Phys. Chem. Chem. Phys.* **18** 3131–6

[8] Truesdell R, Mammoli A, Vorobieff P, Van Swol F and Brinker C J 2006 Drag reduction on a patterned superhydrophobic surface *Phys. Rev. Lett.* **97** 1–4

[9] Gose J W, Golovin K, Tuteja A, Ceccio S L and Perlin M 2016 Experimental Investigation of Turbulent Skin-Friction Drag Reduction Using Superhydrophobic Surfaces *31st Symp. Nav. Hydrodyn.* 11–6

[10] Min T and Kim J 2004 Effects of hydrophobic surface on skin-friction drag *Phys. Fluids* **16** 1–5

[11] Pu X, Li G and Huang H 2016 Preparation, anti-biofouling and drag-reduction properties of a biomimetic shark skin surface *Biol. Open* **5** 389 LP-396

[12] de Lara L R, Jagdheesh R and Ocana J L 2016 Corrosion resistance of laser patterned ultrahydrophobic aluminium surface *Mater. Lett.* **184** 100–3

[13] Lu Z, Wang P and Zhang D 2015 Super-hydrophobic film fabricated on aluminium surface as a barrier to atmospheric corrosion in a marine environment *Corros. Sci.* **91** 287–96

[14] Jagdheesh R, Diaz M and Ocaña J L 2016 Bio inspired self-cleaning ultrahydrophobic aluminium surface by laser processing *RSC Adv.* **6** 72933–41

[15] Vorobyev A Y and Guo C 2015 Multifunctional surfaces produced by femtosecond laser pulses *J. Appl. Phys.* **117**

[16] Ta D V., Dunn A, Wasley T J, Kay R W, Stringer J, Smith P J, Connaughton C and Shephard J D 2015 Nanosecond laser textured superhydrophobic metallic surfaces and their chemical sensing applications *Appl. Surf. Sci.* **357** 248–54

[17] Sun K, Yang H, Xue W, He A, Zhu D, Liu W, Adeyemi K and Cao Y 2018 Anti-biofouling superhydrophobic surface fabricated by picosecond laser texturing of stainless steel *Appl. Surf. Sci.* **436** 263–7

[18] Ferrari M, Benedetti A, Santini E, Ravera F, Liggieri L, Guzman E and Cirisano F 2015 Biofouling control by superhydrophobic surfaces in shallow euphotic seawater *Colloids Surfaces A Physicochem. Eng. Asp.* **480** 369–75

[19] Ou Z, Huang M and Zhao F 2016 The fluence threshold of femtosecond laser blackening of metals: The effect of laser-induced ripples *Opt. Laser Technol.* **79** 79–87

[20] Huang M, Zhao F, Cheng Y, Xu N and Xu Z 2010 The morphological and optical characteristics of micro / nanostructures on GaAs , Si , and brass *Opt. Express* **18** 5694–6

[21] Nayak B K and Gupta M C 2010 Self-organized micro/nano structures in metal surfaces by ultrafast laser irradiation *Opt. Lasers Eng.* **48** 940–9

[22] Rukosuyev M V., Lee J, Cho S J, Lim G and Jun M B G 2014 One-step fabrication of superhydrophobic hierarchical structures by femtosecond laser ablation *Appl. Surf. Sci.* **313** 411–7

[23] Gule N P, Begum N M and Klumperman B 2016 Advances in biofouling mitigation: A review *Crit. Rev. Environ. Sci. Technol.* **46** 535–55

[24] Baharozu E, Soykan G and Ozerdem M B 2017 Future aircraft concept in terms of energy efficiency and environmental factors *Energy* **140** 1368–77

[25] Hansson P M, Swerin A, Schoelkopf J, Gane P A C and Thormann E 2012 Influence of surface topography on the interactions between nanostructured hydrophobic surfaces *Langmuir* **28** 8026–34

[26] Bormashenko E, Stein T, Whyman G, Bormashenko Y and Pogreb R 2006 Wetting properties of the multiscaled nanostructured polymer and metallic superhydrophobic surfaces *Langmuir* **22** 9982–5

[27] Kwon M H, Shin H S and Chu C N 2014 Fabrication of a super-hydrophobic surface on metal using laser ablation and electrodeposition *Appl. Surf. Sci.* **288** 222–8

[28] Chen T, Liu H, Yang H, Yan W, Zhu W and Liu H 2016 Biomimetic fabrication of robust self-assembly superhydrophobic surfaces with corrosion resistance properties on stainless steel substrate *RSC Adv.* **6** 43937–49

[29] Chun D M, Ngo C V and Lee K M 2016 Fast fabrication of superhydrophobic metallic surface using nanosecond laser texturing and low-temperature annealing *CIRP Ann. - Manuf. Technol.* **65** 519–22

[30] Long J, Fan P, Zhong M, Zhang H, Xie Y and Lin C 2014 Superhydrophobic and colorful copper surfaces fabricated by picosecond laser induced periodic nanostructures *Appl. Surf. Sci.* **311** 461–7

[31] Tang M K, Huang X J, Guo Z, Yu J G, Li X W and Zhang Q X 2015 Fabrication of robust and stable superhydrophobic surface by a convenient, low-cost and efficient laser marking approach *Colloids Surfaces A Physicochem. Eng. Asp.* **484** 449–56

[32] Ta V D, Dunn A, Wasley T J, Li J, Kay R W, Stringer J, Smith P J, Esenturk E, Connaughton C and Shephard J D 2016 Laser textured superhydrophobic surfaces and their applications for homogeneous spot deposition *Appl. Surf. Sci.* **365** 153–9

[33] Steele A, Nayak B K, Davis A, Gupta M C, Loth E, Adam S, Barada K N, Alexander D, Mool C G and Eric L 2013 Linear abrasion of a titanium superhydrophobic surface prepared by ultrafast laser microtexturing *J. Micromechanics Microengineering* **23** 115012

[34] Wu B, Zhou M, Li J, Ye X, Li G and Cai L 2009 Superhydrophobic surfaces fabricated by microstructuring of stainless steel using a femtosecond laser *Appl. Surf. Sci.* **256** 61–6

[35] Li B, Li H, Huang L, Ren N and Kong X 2016 Femtosecond pulsed laser textured titanium surfaces with stable superhydrophilicity and superhydrophobicity *Appl. Surf. Sci.* **389** 585–93

[36] Martínez-Calderon M, Rodríguez A, Dias-Ponte A, Morant-Miñana M C, Gómez-Aranzadi M and Olaizola S M 2016 Femtosecond laser fabrication of highly hydrophobic stainless steel surface with hierarchical structures fabricated by combining ordered microstructures and LIPSS *Appl. Surf. Sci.* **374** 81–9

[37] Cunha A, Serro A P, Oliveira V, Almeida A, Vilar R and Durrieu M C 2013 Wetting behaviour of femtosecond laser textured Ti-6Al-4V surfaces *Appl. Surf. Sci.* **265** 688–96

[38] Bizi-Bandoki P, Valette S, Audouard E and Benayoun S 2013 Time dependency of the hydrophilicity and hydrophobicity of metallic alloys subjected to femtosecond laser irradiations *Appl. Surf. Sci.* **273** 399–407

[39] Kietzig A M, Hatzikiriakos S G and Englezos P 2009 Patterned superhydrophobic metallic surfaces *Langmuir* **25** 4821–7

[40] Sarbada S and Shin Y C 2017 Superhydrophobic contoured surfaces created on metal and polymer using a femtosecond laser *Appl. Surf. Sci.* **405** 465–75

[41] Jagdheesh R, Pathiraj B, Karatay E, Römer G R B E and Huis In'T Veld A J 2011 Laser-induced nanoscale superhydrophobic structures on metal surfaces *Langmuir* **27** 8464–9

[42] Long J, Zhong M, Zhang H and Fan P 2015 Superhydrophilicity to superhydrophobicity transition of picosecond laser microstructured

aluminum in ambient air *J. Colloid Interface Sci.* **441** 1–9

[43] Liu B, Wang W, Jiang G, Mei X, Wang Z, Wang K and Cui J 2016 Study on hierarchical structured PDMS for surface super-hydrophobicity using imprinting with ultrafast laser structured models *Appl. Surf. Sci.* **364** 528–38

[44] Yang Y, Yang J, Liang C and Wang H 2008 Ultra-broadband enhanced absorption of metal surfaces structured by femtosecond laser pulses *Opt. Express* **16** 11259–65

[45] Tang M, Shim V, Pan Z Y, Choo Y S and Hong M H 2011 Laser ablation of metal substrates for super-hydrophobic effect *J. Laser Micro Nanoeng.* **6** 6–9